Materials Science Forum
ISSN: 1662-9752, Vol. 1012, pp 296-301
doi:10.4028/www.scientific.net/MSF.1012.296

Submitted: 2020-07-29
Accepted: 2020-08-04
Online: 2020-10-27

Effect of Post-Weld Heat Treatment on Hardness in Superduplex Stainless Steel ASTM A890/A890M - Grade 6A

Clélia Ribeiro de Oliveira[1a *], Eloá Lopes Maia[1b], Solange Tamara da Fonseca[1c], Marcelo Martins[2d], Julián Arnaldo Ávila Díaz[3e], Paulo Roberto Mei[1f]

[1]UNICAMP, Rua Mendeleyev-200, CEP 13083-860, Campinas/SP, Brasil

[2]UNISAL, Rua Dom Bosco-100, CEP 13466-327, Americana/SP, Brasil.

[3]UNESP, Av. Profa. Isette Corrêa Fontão-505, CEP 13876-750, São João da Boa Vista/SP, Brasil

[a*]clelia19@fem.unicamp.br, [b]eloamaia@gmail.com, [c]solange.tamara.fonseca@gmail.com, [d]marcelovarellamartins@gmail.com, [e]julian.avila@unesp.br, [f]pmei@fem.unicamp.br

Keywords: Superduplex stainless steels, ASTM A890/A890M standard, post-welded heat treatment, Vickers hardness.

Abstract. Superduplex stainless steel alloy exhibit high mechanical and corrosion resistance, which main industrial application is in the petrochemical industry. The manufacture and maintenance of such equipment usually involve welding processes, followed by post-welded heat treatment and it often becomes impossible to apply heat treatments. Thereby, the purpose of this work is to verify the effect of a post-welded heat treatment on shielded metal arc welding in steel grade ASTM A890/A890M - grade 6A. The microstructure in the as-welded condition consisted of austenite, secondary austenite, and ferrite phases and, the post-welded heat treatment condition exhibited only austenite and ferrite. The hardness in the melt zone reached values of 300 HV after welding and, the value was reduced to 260 HV in the post-welded heat treatment condition.

Introduction

The superduplex stainless steels (SDSS) are classified as materials having a PREN (Pitting Resistance Equivalent Number) above 40 [1] it is meaning a high resistance to corrosion, and also presents high mechanical strength [2]. A good combination of properties is reached when the volumetric fractions of the ferrite (δ) and austenite (γ) phases are around 50/50 [3,4]. Welding in these materials is an important factor to be considered since the high temperatures achieved associated with a rapid cooling can alter volumetric fractions of the ferrite and austenite phases, as well as promote the formation of undesirable phases such as chromium nitrides, carbides, and sigma. Low levels of ferrite (<25%) or high (>75%) may lead to decreased mechanical properties and corrosion resistance [5]. Ferrite has a higher hardness than austenite; 288 and 270 HV, respectively [6], in nanoindentation techniques in duplex stainless steels the ferrite phase presents higher values of mechanical resistance than the austenite phase [7]. In addition, Cr and Mo presence increase the hardness at the ferrite phase[8].

The microhardness measurement in welded joints is one of the main characterization techniques providing information of the hardness profile along the 3 zones, base metal (BM), heat-affected zone (HAZ) and fusion zone (FZ). In general, the volumetric fraction of ferrite is much larger than that of austenite in FZ and HAZ. The rapid heating and cooling cycles cause the HAZ and FZ in the SDSS to exhibit excessive ferritization, increasing the hardness of the same.

Post-welded heat treatments (PWHT) promote the return of ferrite and austenite volumetric fractions to levels close to 50/50, in addition to reducing residual stress caused by welding [9]. To obtain an ideal phase balance, several studies have focused on PWHT in welded joints in SDSS [10]. Although this process is effective in eliminating excessive welding in SDSS welded areas, it is not practical to perform PWHT for welding in large areas. In this work, the effect of PWHT on the hardness of welded regions of ASTM A890/A890M - grade 6A steel was investigated.

Experimental Procedure

Plates of SDSS steel 6A, ASTM A890/A890M standard, supplied by SULZER BRASIL S.A. were used in the present study. The alloy was produced in an induction furnace with Vacuum Induction Melting (VIM), with a maximum power of 400 kW and a frequency of 60 Hz. The plates were solidified in sand molding in the dimensions 360x110x40 mm., after being thermally treated at the temperature according to the established by the standard ASTM A890/A890M.

The addition metal during welding was the AISD Zeron®100, its chemical composition is close to BM, as shown in Table 1. Shielded Metal Arc Welding (SMAW), double V-bevel and 70° angle with approximately 90 passes, the voltage was between 20 - 25 V and the current was between 100 - 130 A.

Table 1. Chemical Compositions and PREN* of ASTM A890/A890M - grade 6A and Zeron®100 electrodes (wt%)

	C	P	S	Cr	Ni	Mo	Cu	W	N	PREN
6A	0.023	0.025	0.005	25.13	8.22	3.53	0.89	0.67	0.29	41.4
Zeron®100	0.028	0.029	0.006	25.1	8.06	4.19	0.42	0.44	0.26	43.1

*PREN = %Cr+3.3%Mo+16%N≥40 (% by weight).

After the welding procedure, part of the welded plates was cut to conduct the PWHT at 1140 °C for 4 h with subsequent cooling in water. For microstructural analysis, the cross-section of the welds was prepared by the grinding and polishing procedure. Sandpaper with 320 to 1200 mesh was used in the first stage and finished with polishing using the diamond paste of 6 μm, 3 μm and 1 μm. Electrolyte etching was conducted with 3 volts for 15 seconds in a 20% aqueous solution of NaOH. The images were obtained by light optical microscope (LOM), model EVO-MA15 and software for acquisition of Axiovision 4.8.2 images.

The microhardness map was obtained through an automated LECO AMH43 system with Vickers indenter using load of 2.94 N (300 kgf - 3000 gf) and loading time of 15 seconds, according to ASTM E384 standard [11] and spacing 200 μm as shown in Fig.1. To establish the hardness distribution within the weld, indentations were located at the BM, HAZ, and FZ as depicted in Fig. 1. The hardness data were processed using the Microcell software and colored maps were produced according to the hardness intensity through the cross-section.

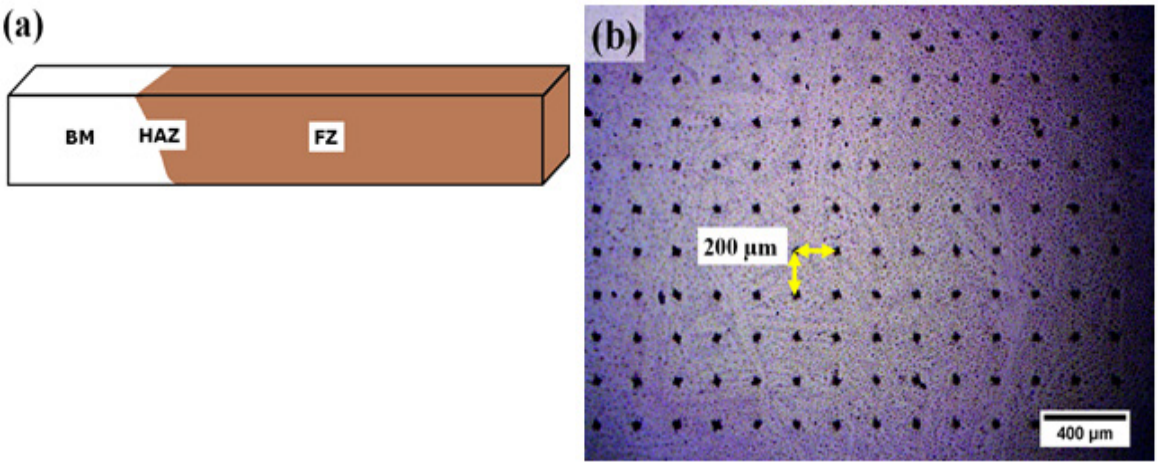

Fig. 1: a) Schematic drawing of the region of the weld where the microhardness map was performed and in b) is described.

Results and Discussion

The ferrite (δ) and austenite (γ) phases were observed in the conditions as-welded and with PWHT as shown in Fig. 2. In the as-welded condition, the precipitation of secondary austenite (γ_2) was observed, which was subsequently dissolved PWHT. The formation of secondary austenite

occurs mainly in the region between the passes due to the temperature experienced during welding. Since high temperatures and then abrupt cooling occurs, ferrite saturation of austenite stabilizing elements such as Ni may occur, and during cooling or subsequent passes, a localized precipitation of small austenite grains, known as secondary austenite (γ_2) occurred [3].

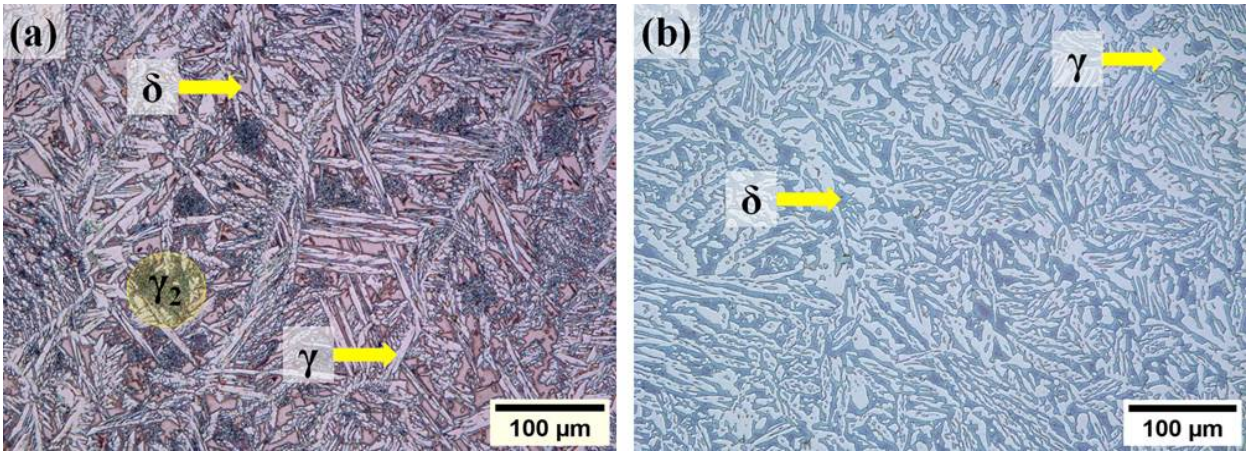

Fig. 2: FZ microstructure: a) as-welded; b) PWHT. Electrolytic etching with 20% NaOH. LOM.

In the microhardness test, it was observed that the PWHT uniformized of the hardness in the regions of the BM, HAZ, and FZ, according to Fig. 3. The high hardness was observed between passes, as indicated by the arrows in Fig. 3 in the as-welded conditions and PWHT these regions have the lower hardness.

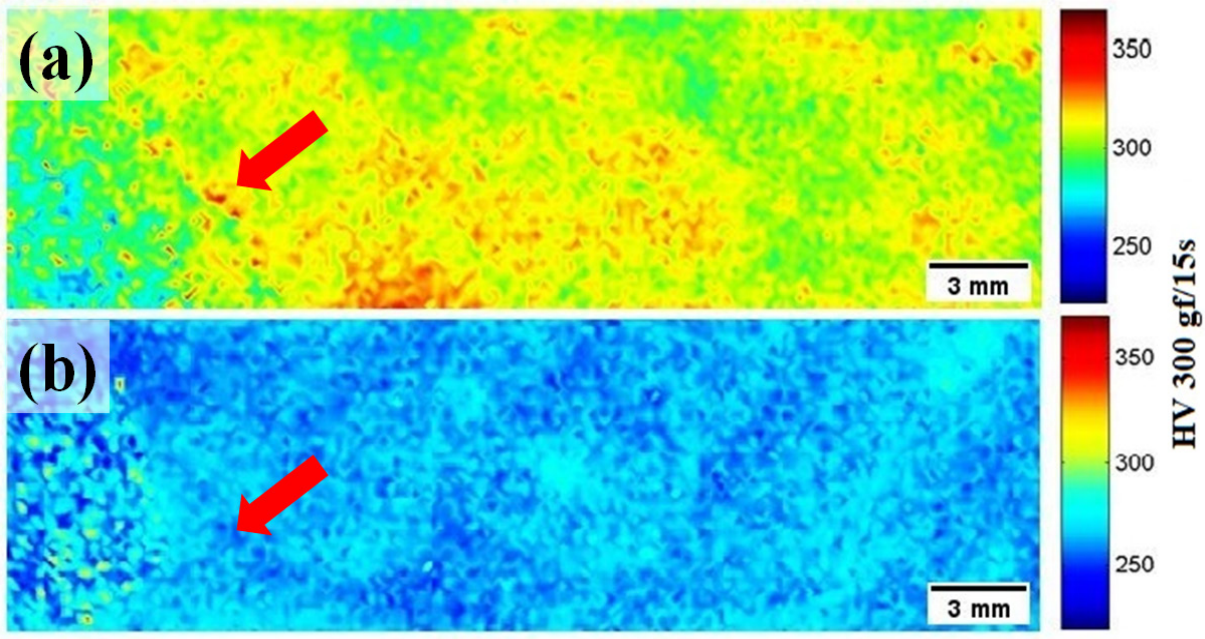

Fig. 3: Hardness maps of the a) as-welded and b) PWHT conditions.

Fig. 4 and 5 show the hardness profile along the BM, HAZ, and FZ regions (cross-sectional and longitudinal). In the as-welded condition the average hardness at the intersection of the yellow lines was around 307 HV, as shown in Fig. 4, by the hardness profile in the BM were found the lowest hardness indexes and in the FZ values most taken. PWHT, the highest hardness peaks were concentrated in the BM and in the solder with lower values and more uniform with a mean of 268 HV, see Fig. 5. These results are strongly related to the adjustment of the ferrite and austenite phases and the partition of the elements of turns on.

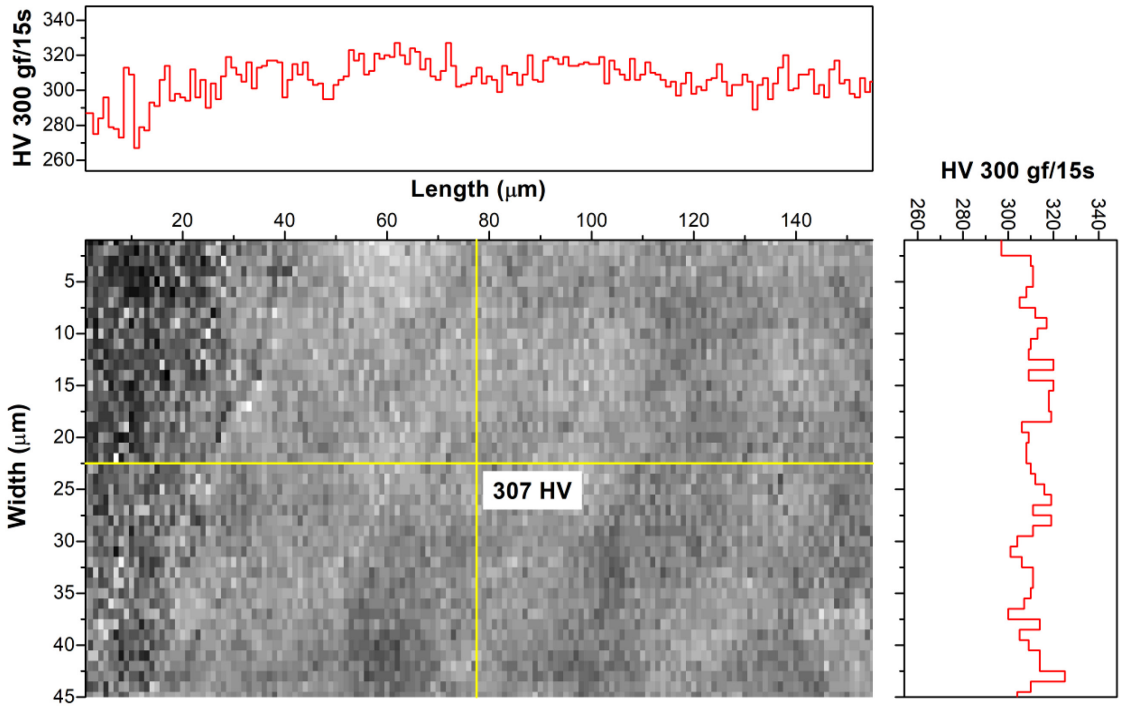

Fig. 4: Hardness maps and line profiles in the as-welded condition (yellow lines).

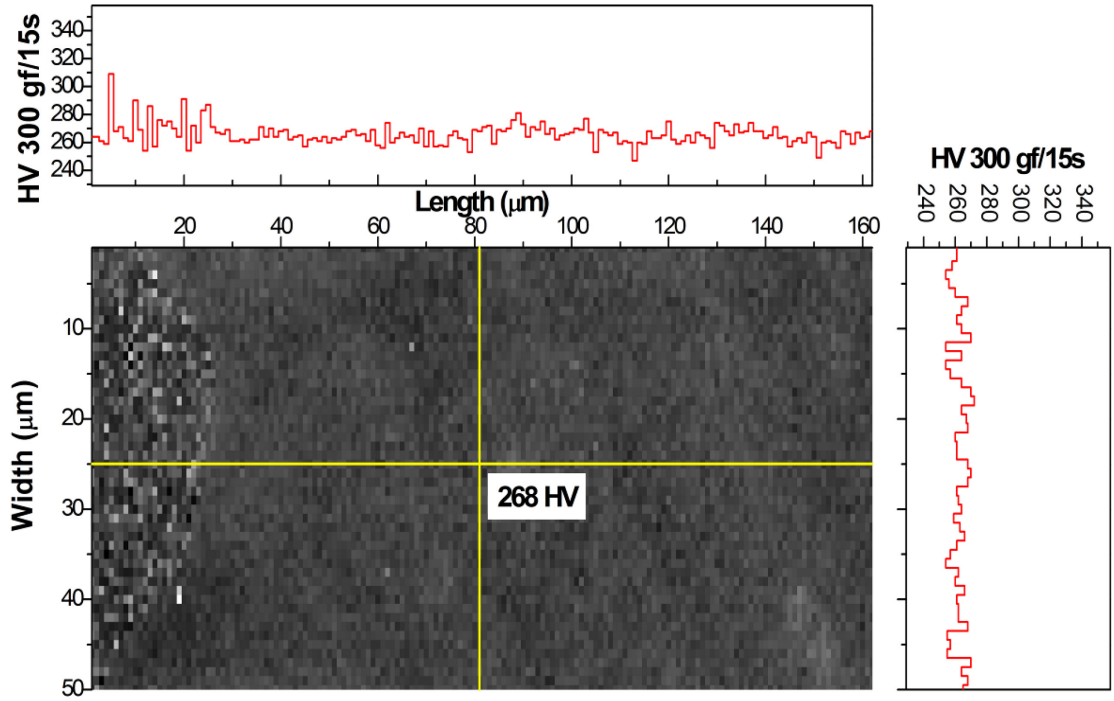

Fig. 5: Hardness maps and line profiles in the PWHT condition (yellow lines).

In the histogram shown in Fig. 6, the highest values of hardness frequency for the 6A steel in the as-welded condition was around 300 HV to 320 HV and reduced in the PWHT condition between 260 HV to 280 HV. Hence, austenite has lower hardness values when compared to ferrite, and the ferrite prior to PWHT condition may be saturated with austenite stabilizing alloying elements, this causes an increase in the hardness of the steel, as it hinders the movement of the mismatches during mechanical stresses.

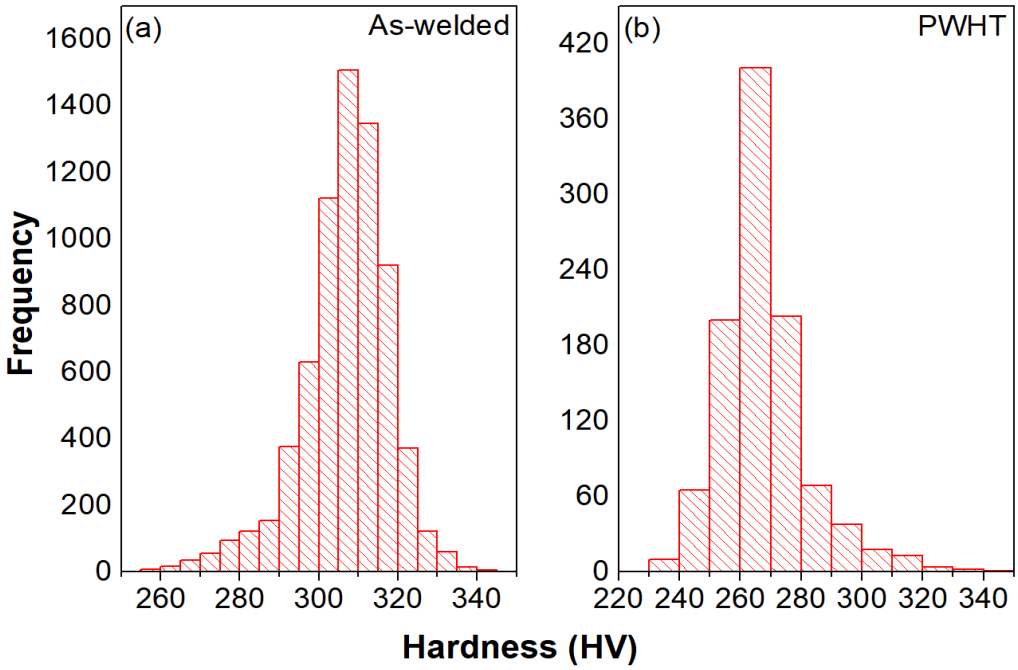

Fig. 6: Hardness histogram of 6A steel of the a) as-welded and b) PWHT conditions.

Conclusions

The analysis of the hardness in SDSS grade 6A in the as-welded and PWHT condition allowed to obtain some conclusions, such as:

- In the metallographic analysis were found ferrite, austenite and austenite secondary phases in the as-welded and PWHT conditions. The as-welded condition presented an unbalance of the phases, however, after the PWHT there was an adjustment of the phases to only ferrite and austenite.
- After the PWHT the hardness in the FZ was uniform with the BM and decreased from 300 HV for 260 HV;

Acknowledgment

The authors would like to thank LNNano/CNPEM for the use of the durometer Future-Tech FV 800 model, the FEM/UNICAMP, the Conselho Nacional de Desenvolvimento Cientifico e Tecnológico (CNPq) – process number 142260/2016-9, the Espaço da Escrita – Pró-Reitoria de Pesquisa – UNICAMP - for the language services provided and SULZER BRASIL S.A. by the material supply.

References

[1] ASTM A890/A890M - 13, Standard Specification for Castings, Iron-Chromium-Nickel-Molybdenum Corrosion- Resistant, Duplex (Austenitic/Ferritic) for General Application1, ASTM Int., 01.02 (2014) 1–5.

[2] S. Atamert, J.E. King: Mater. Sci. Technol. Vol. 8 (1992), p. 896.

[3] J. Charles: Rev. Métallurgie Vol. 105 (2008), p. 5.

[4] J.O. Nilsson: Mater. Sci. Technol. Vol. 8 (1992), p. 685.

[5] A.I. Mourad, A. Khourshid, T. Sharef: Mater. Sci. Eng. A Vol. 549 (2012), p. 105.

[6] J.D. Kordatos, G. Fourlaris, G. Papadimitriou: Mater. Sci. Forum Vols. 318–320 (1999), p. 615.

[7] K.R. Gadelrab, G. Li, M. Chiesa: J. Mater. Res. (2012). DOI: 10.1557/jmr.2012.99

[8] A. Vinoth Jebaraj, L. Ajaykumar, C.R. Deepak, K.V.V. Aditya: J. Adv. Res. Vol. 8 (2017), p. 183.

[9] P. Dong, S. Song, J. Zhang: Int. J. Press. Vessel. Pip. Vol. 122 (2014), p. 6.

[10] Z. Zhang, H. Zhang, J. Hu, X. Qi, Y. Bian, A. Shen, P. Xu, Y. Zhao: Constr. Build. Mater. Vol. 168 (2018), p. 338.

[11] ASTM E384 - 11, Standard Test Method for Knoop and Vickers Hardness of Materials, ASTM Int. (2012) 1–43.